Xiaobo Yang[1], Yijun He[1*]

[1] School of Marine Sciences, Nanjing University of Information Science & Technology, Nanjing, China.

Corresponding author: Yijun He (yjhe@nuist.edu.cn)

Key Points:

- The differences between the satellite's velocity measured from the Doppler centroid and the velocity measured by the Doppler centroid anomaly are compared in detail, and the imaging mechanism is investigated.
- The concept of radial velocity is clearly revealed.

Abstract

The concept of radial velocity is proposed for high frequency (HF) radar for sea surface current measurement. However, in a spaceborne synthetic aperture radar (SAR) system, the meaning of this concept has changed greatly. Through the evidence and analysis presented in this paper, the radial velocity of the sea surface observed via spaceborne SAR is revealed from the projection of the satellite's velocity at different points along the range direction, and its distribution on the image presents a strip-like texture, which is very different from the central radial distribution on the velocity image measured via HF radar. The retrieved sea surface velocity field does not exhibit any radial characteristics, and its value is solely the magnitude of the sea surface velocity.

Plain Language Summary

Spaceborne SAR and HF radar are two instruments for detecting the sea surface current field. Research on HF radar began much earlier than research on spaceborne SAR, so it is generally believed that the velocity measured via spaceborne SAR is also the radial component of the sea surface velocity, which is consistent with the radial sea surface velocity measured via HF radar. Through sufficient evidence, in this paper, it is shown that the sea surface velocity measured via spaceborne SAR is not the radial velocity but rather the magnitude of the sea surface velocity. Only the range satellite velocity measured via spaceborne SAR presents a strip-like radial feature. Based on the explanation presented in this paper, spaceborne SAR will become the most important technique for sea surface current remote sensing since it can directly obtain the velocity field of the sea surface current.

1 Introduction

In the previous article, we proposed an effective scheme for Ekman current retrieval, but the problem regarding the radial velocity was not clearly explained due to the limited focus of that article. Thus, in this paper, we discuss the problem of the radial velocity, including the concept of the radial velocity, the Doppler radial velocity measured via satellite, and the difference between the

radial velocity measured via satellite and the sea surface velocity measured from the Doppler centroid anomaly (DCA).

Regarding the history of the concept of the radial velocity, Crombie (1955) first discovered the Doppler frequency shift caused by the Bragg wave and pointed out that the Doppler velocity measured using ground-based radar is the radial ocean wave velocity, i.e., the wave velocity along the direction of the radar beam. Then, the Doppler spectrum theory began to be considered. Wait (1966) showed that the peak of the Doppler-echo spectrum corresponds to the height of the Bragg-resonant wave-train. Barrick (1972a, b) proposed first-order and second-order models of the Doppler spectrum. Following this, the statistical characteristics of the sea-echo Doppler spectrum were clearly revealed (Barrick & Snider, 1977). Based on this deep understanding of the Doppler spectrum, Barrick (1977) invented a technique for measuring the sea surface radial currents using high frequency (HF) radar and established the concept that the sea surface current measured via radar is only the radial velocity of the current. Then, Lipa and Barrick (1983) composed the sea surface current vector using the radial velocity in the Coastal Ocean Dynamics Applications Radar (CODAR) system using the least squares method. After this, researchers began to believe that the sea surface velocity measured via radar is the radial velocity of the sea surface current.

In 1978, Barrick summarized the application of HF radar in oceanography, which was the beginning of the application of radar in oceanography. In the same year, the National Oceanic and Atmospheric Administration (NOAA) launched the first spaceborne synthetic aperture radar (SAR) satellite, SeaSat, based upon which the range Doppler algorithm was proposed for processing the SAR images. In 1955, Carl Wiley discovered that the resolution of the imaging radar could be increased through the Doppler shift, and therefore, the concept of synthetic aperture radar was invented. In 2002, Chapron found that the Doppler centroid anomaly (DCA) extracted from the Doppler centroid (DC) can be used for sea surface current retrieval (Romeiser et al., 2010). Chapron et al. (2005) called the velocity measured by the DCA the line-of-slight velocity in their paper, and later Johannessen et al. (2006) called it the radial velocity in a conference paper. Johannessen et al. (2008) formally used the term radial velocity in their paper published in *Geophysical Research Letters*. Researchers have treated the velocity measured using the DCA as the radial velocity, which is mostly due to Barrick's brilliant work. However, a basic difference is that the SAR satellite is located in space, while HF radar is located on the ground (also called ground-state HF radar). This difference makes the velocity measured by the spaceborne SAR system very different from the velocity measured by the HF radar system. We explain the reason for this in detail in this paper.

2 Radial Doppler satellite velocity

In the previous article (Yang & He, 2022) , we explained the composition of the DC. Although the DC contains the error term introduced by the Doppler centroid estimation algorithm, the error term can be ignored compared with

the Doppler shift caused by the satellite's motion and sea surface motion when analyzing the radial characteristics of the DC. Thus, we can express the DC as follows:

$$f_{\mathrm{DC}} = f_{\mathrm{SAT}} + f_{\mathrm{DCA}}. \quad (1)$$

The satellite motion component f_{SAT} is much larger than the sea surface motion component f_{DCA}, so the DC frequency f_{DC} mainly exhibits the characteristics of the f_{SAT}. Both theoretical analysis (Cumming & Wong, 2004) and real-data analysis (Wang et al., 2022) have shown that the f_{SAT} has significant radial characteristics. Figure 1 shows the linear trends of the f_{DC} in both the azimuth and range directions. Based on this linear trend, we can identify and analyze the radial features of the f_{SAT}.

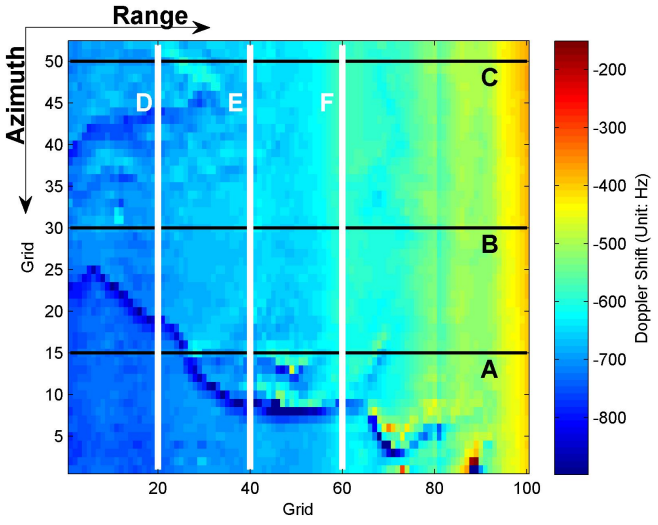

(a)

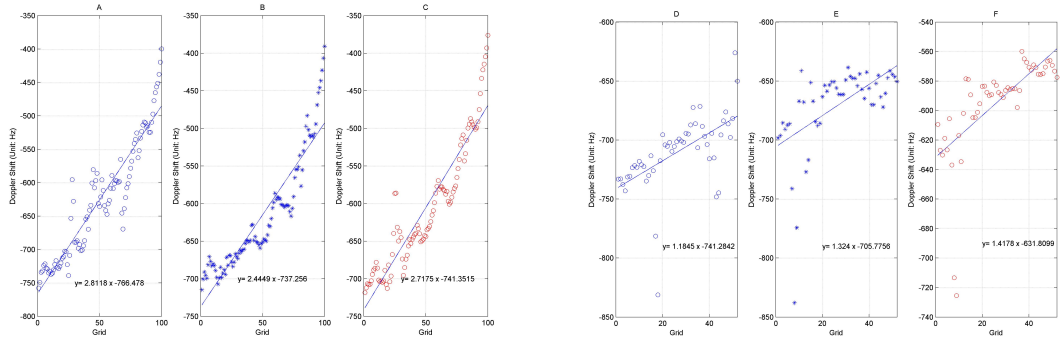

(b) (c)

Figure 1. The linear trend of the Doppler centroid frequency f_{DC}. (a) The f_{DC} image derived from the Environmental Satellite (ENVISAT) advance synthetic aperture radar (ASAR) mapping on 07/14/2007 at Hangzhou Bay, with three profiles A, B and C along the range direction and three profiles D, E and F along the azimuth direction.. The linear trends of the profiles along the (b) range and (c) azimuth directions.

2.1 Linear trend of Doppler shift

As shown in Figure 1, the linear trend of the DC in the range direction (Figure 1b) is quite different from that in the azimuth direction (Figure 1c). The slopes of the linear trend profiles in the range direction are not equal to each other but almost around 2.6, which means that the imaging patterns of the DC in different places in range direction are not different, even though the satellite velocities in these places are significantly different. Since the satellite's speed is much greater than the sea surface speed, $f_{\mathrm{SAT}} \gg f_{\mathrm{DCA}}$, so $f_{\mathrm{DC}} \cong f_{\mathrm{SAT}}$. Thus, the profiles shown in Figure 1 illustrate that the f_{SAT} changes linearly in both the azimuth and range directions. Wang et al. (2022) developed two DC models to describe the linear trends in the azimuth and range directions over the sea surface. However, these two models were constructed from the geometry of the satellite's motion, so they essentially describe the f_{SAT}, not the f_{DC}. Even over land, the f_{DC} is still not completely equal to the f_{SAT} because, as mentioned in our previous article,

$$f_{\mathrm{DC}} = f_{\mathrm{SAT}} + f_{\mathrm{topo}}, \quad (2)$$

where f_{topo} is the DC frequency induced by the terrain variations, and $f_{\mathrm{SAT}} \gg f_{\mathrm{topo}}$. Equations (1) and (2) both contain the Doppler shift components independent of the satellite's motion, and these components cannot be described by the DC models provided by Wang et al. (2022). Thus, to be more precise, the DC model in the range direction can be rewritten as follows:

$$f_{\mathrm{DC}}^{\mathrm{Rg}} = f_{\mathrm{SAT}}^{\mathrm{Rg}} + f_{\mathrm{DCA}},$$

$$f_{\mathrm{SAT}}^{\mathrm{Rg}} = f_0 + f_0 \frac{\cos\varphi_0}{(sin\ \varphi_0)^2}\left(\frac{\cos\varphi_0}{R_0} - \frac{1}{H}\right)(R - R_0), \quad (3)$$

where f_0 is constant for an instantaneous scene, R is the slant distance, and R_0 is the slant distance corresponding to the same instantaneous scene. $_0$ and H are also constant for the same scene. The theoretical range model $f_{\mathrm{SAT}}^{\mathrm{Rg}}$ indicates that the linear trend in the range direction is correlated with the range distance. Taking profile A as an example, when the satellite transmits and receives electromagnetic signals above the sub-satellite point corresponding to A, the time lag of this procedure is extremely short, so the satellite's speed in the instantaneous azimuth direction can be considered to be uniform. Therefore, f_0 is a constant and $f_{\mathrm{SAT}}^{\mathrm{Rg}}$ is only related to the range distance. This is the reason why the profiles of the DC in the range direction are linearly correlated with the range distance.

For the azimuth direction, the slopes of the linear trend profiles are about 1.3,

far different from that of the range direction, which indicates that the imaging pattern of the f_{SAT} in the azimuth direction is completely different from the pattern in the range direction. The theoretical azimuth DC model can be express as follows:

$$f_{\mathrm{DC}}^{\mathrm{Az}} = \quad f_{\mathrm{SAT}}^{\mathrm{Az}} + f_{\mathrm{DCA}},$$

$$f_{\mathrm{SAT}}^{\mathrm{Az}} = -\frac{2}{\lambda|\mathbf{R}|}\mathbf{VR} = -\frac{2}{\lambda|\mathbf{R}|}\mathbf{V^2}t, \quad (4)$$

where $\mathbf{V}$ is the satellite's velocity, $\mathbf{R}$ is the vertical distance of the satellite from the Earth's surface, and t is time. Based on Equation (4), we know that $f_{\mathrm{SAT}}^{\mathrm{Az}}$ is mainly affected by the changes in the satellite's speed. The swath of a SAR image is about 200 km, while the circumference of the Earth is about 40075 km, so the ratio of the imaging area to the circumference of the Earth is about 0.5%. Using this ratio, we can treat the change in the satellite's speed along the orbit as a linear process instead of a circular motion process because the change in the curvature of the satellite's orbit for this ratio can be neglected. We conclude that the f_{SAT} trend in the azimuth direction is mainly caused by the linear change in the satellite's speed.

To illustrate the f_{SAT} differences in the different directions more intuitively, we obtained the linear trends of the images of the f_{SAT} in the azimuth and range directions using the linear fitting method (Figure 2) (Wang et al., 2022).

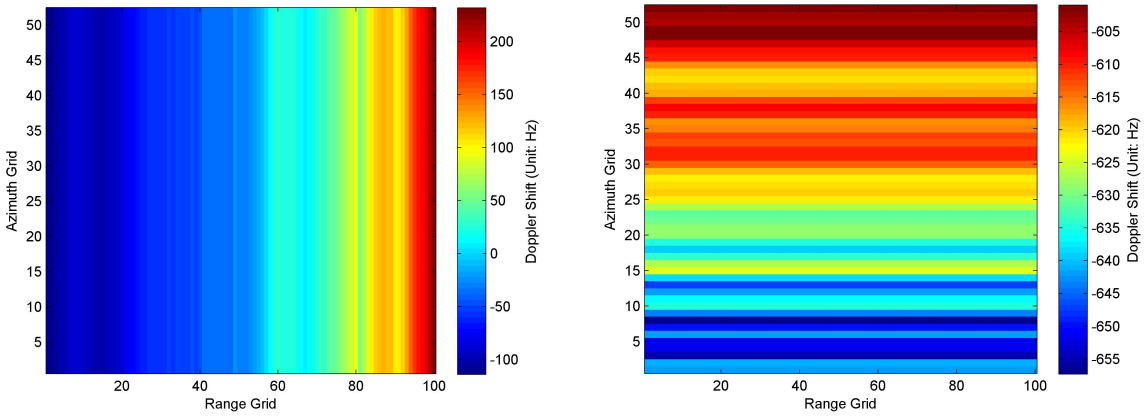

(a) (b)

Figure 2. The linear trends of the images of the f_{SAT} in different directions. (a) The $f_{\mathrm{SAT}}^{\mathrm{Rg}}$ image, with clear vertical strips. (b) The $f_{\mathrm{SAT}}^{\mathrm{Az}}$ image with horizontal stripes.

2.2 Radial features of the Doppler satellite velocity

Because the Doppler shift is linearly correlated with the velocity, i.e., $f = \frac{k}{2\pi}v$, where k is a constant representing the electromagnetic wave number. Thus, in this section, the satellite-induced Doppler shift image will replace the satellite velocity image to analyze the radial characteristics of the Doppler satellite velocity. As shown in Figure 2, the radial feature of the f_{SAT} can be easily identified, that is, the range image shown in Figure 2a exhibits significant linear characteristics. These radial features are not revealed in Figure 2b. One reason for this is that the linear trends in the azimuth direction are only related to the satellite's speed, not to the projection of the radar beam. The other reason is that the beams of the radar are emitted only along the range direction. Radial features can only be found along the range direction. The linear characteristics are closely related to the range distance, which is simply the projection feature of the electromagnetic wave signal in the range direction.

By comparing the radial features in Figure 2a with the case study of HF radar presented by Mujiasih et al. (2021), it was found that the distribution of the radial velocity measured via HF radar on the image (Figure 9 in Mujiasih et al., 2021) is different from the distribution of the radial Doppler velocity measured via satellite. For the radial velocity measured via HF radar, the distribution texture is circumferential and radial. However, in Figure 2a, the SAR-measured radial velocities exhibit a striped distribution. These distribution differences are due to the synthetic aperture mechanism (Figure 3). Within a single synthetic aperture length in the two-dimensional signal storage space, a stationary target is observed in motion and is expressed as echo signals in the black box area. This also leads to the range cell migration (RCM) disproportionately shown as the black curve in the box (Cumming & Wong, 2004). The echo energy of a single target usually covers hundreds of samples in the range and azimuth directions, while the RCM may only span several range sampling units, so Figure 3 is not drawn disproportionately. The echo signals are stored using the range and azimuth directions as the coordinate axes, so the DC values are also estimated and stored in two dimensions using the range and azimuth coordinates. This causes the range and azimuth characteristics of the f_{SAT} to be distributed in strips.

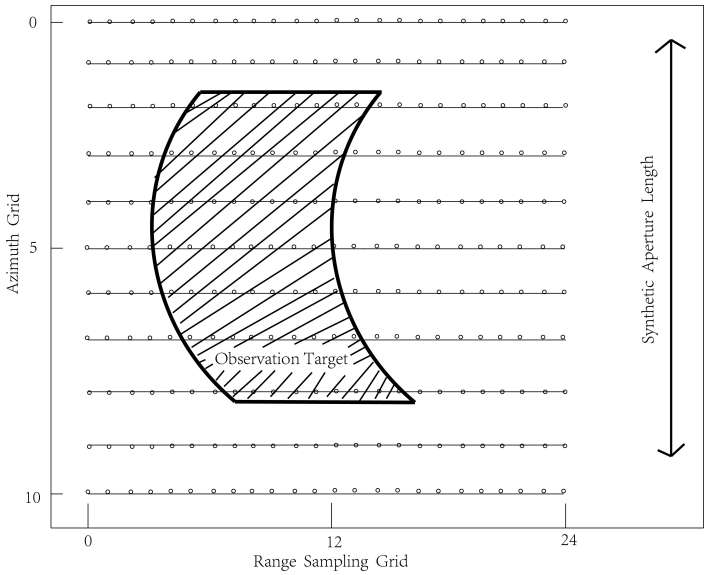

Figure 3. The synthetic aperture mechanism in the two-dimensional signal storage space. The range and azimuth directions are taken as the coordinate axes in this space.

More importantly, the SAR measured sea surface velocity is essentially different from the radial sea surface velocity measured via HF radar. This is discussed in the next section.

3 Sea surface Doppler velocity

For the retrieval of the sea surface velocity from the DC, Wang et al. (2022) provided an effective algorithm with a reasonable validation. In this section, we continue to use the Doppler shift image instead of the sea surface velocity image to analyze the radial features of the distribution on the retrieved sea surface velocity image. On the image of the f_{DCA}, two profiles are also created along the azimuth and range directions respectively (Figure 4). Regarding these profiles, there are no clear linear trends similar to the satellite radial velocity in both the range and azimuth directions. Moreover, the distribution of the values on the f_{DCA} image does not exhibit a striped texture, and the distribution is more similar to the dynamic features of the sea surface. In the previous article, we also proved that the sea surface velocities measured via SAR are approximately equal to or even greater than the velocities simulated using a numerical model. All of these lines of evidence obtained from real data prove that the sea surface velocity retrieved from the DC is exactly equal to the magnitude of the sea surface vector, not the magnitude of the radial component of the vector.

So, why is the sea surface velocity measured via SAR so different from that measured via HF radar? In the previous article, we partially explained the reason for this phenomenon and proposed a new imaging mechanism for the f_{DCA}.

One of the main conclusions is that the electromagnetic wave signals emitted by the SAR system in space are dispersed in the long-distance propagation and projected onto the sea surface to form concentric ellipses, so it can observe the Doppler shift in any velocity direction. In contrast, the electromagnetic wave emitted by an HF radar system on the ground has good radial propagation characteristics, so the measured velocity is simply the radial speed of the sea surface velocity. Here, we use an example to clearly illustrate that the electromagnetic wave dispersion caused by the long-distance transmission greatly affects the measurement of the sea surface velocity. This example was presented by Martin et al. (2022), and they compared the measured velocities of the Sentinel-1 RVL product with the radial velocity measured via HF radar in the near shore region and far sea region. The scatter plot presented in Figure 4 of their article shows that in the near shore area, the SAR measured velocities were generally larger than the radial velocities from the HF radar; in the far sea area, the velocities obtained via SAR were approximately equal to the radial velocities measured via HF radar. Since it has been proven in the previous article that the SAR measured velocity is only the magnitude of the sea surface vector, we can infer that the electromagnetic wave emitted by the HF radar is also dispersed in the far sea area, leading to its radial features no longer being significant. In addition, the measured velocity gradually changes from the radial direction to a non-radial direction. This example also demonstrates that the SAR measured sea surface velocity is not the radial velocity due to the dispersion effect of the electromagnetic waves after transmission over several hundred kilometers.

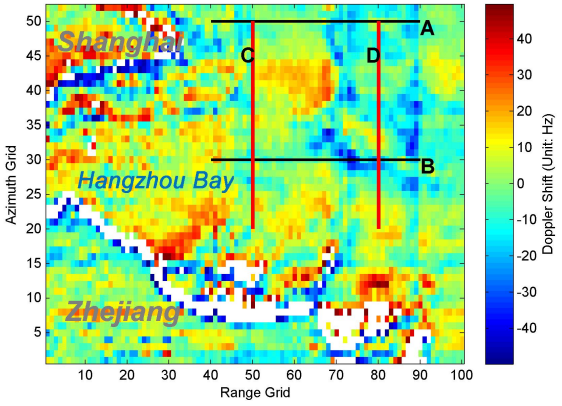

(a)

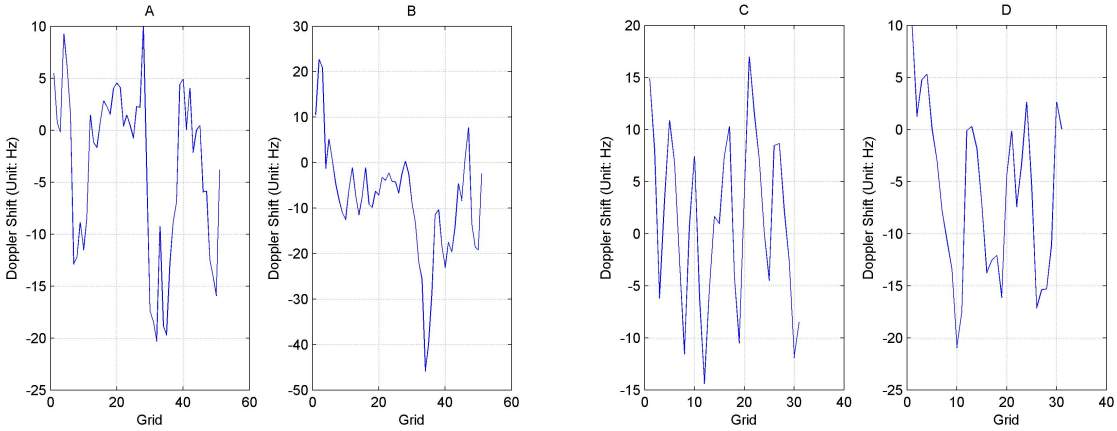

(b) (c)

Figure 4. DCA image retrieved from the DC image and its profiles. (a) The f_{DCA} image with two profiles A and B along the range direction and two profiles C and D along the azimuth direction. The abnormal values shown in white color are due to the great differences of electromagnetic wave scatter between sea water and land. (b) The trends of the two profiles along the range direction. (c) The trends of the two profiles along the azimuth direction.

A surprising fact is that both the sea surface velocity and the satellite's velocity are measured at the same time using the Doppler effect, but only the measured satellite velocity is radial in the range direction, while the sea surface velocity is not radial. To explain this, we can merely focus on the observation points in range direction. First, We select two points (A and B) at certain distances along the range direction and observe the values of the sea surface velocity and the satellite's speed at these two points. We assume that the satellite's velocity V remains constant in the very short time period of the sampling in range direction. The measured velocity at point A contains the sea surface velocity $\mathrm{U_A}$ at point A and the component satellite velocity $\mathrm{V_A}$, while that at point B contains the sea surface velocity $\mathrm{U_B}$ at point B and the component satellite velocity $\mathrm{V_B}$. Then we can find that only $\mathrm{V_A}$ and $\mathrm{V_B}$ are radially correlated through Equation (3). $\mathrm{U_A}$ is quantitively not related to $\mathrm{U_{B,}}$ since SAR just samples the sea surface velocity point-to-point and the sea surface velocity is different at different points. This can explain why only the measured satellite velocity is radial.

A related question is if the same sea surface point is observed at two different points in the azimuth and range directions, is there a radial relationship between the two observation velocities? To answer this, we checked the Doppler velocity images of the extension region of the Gulf Stream and the Gulf Stream regime (Figure 5). A uniform sea surface current field can be seen on the image, with a flow direction that almost corresponds to the range direction of the SAR (Figure

5a). From the profile along the black line in Figure 5c, we can see that no radial feature is found at the different observation points along the range direction for the same current area. The Doppler velocity image of the Gulf Stream regime (Figure 5b) provides the same conclusion along the azimuth direction in Figure 5d. Thus, based on Figure 5, we know that the measured speeds at the same sea surface field at different positions along the satellite's orbit are the same.

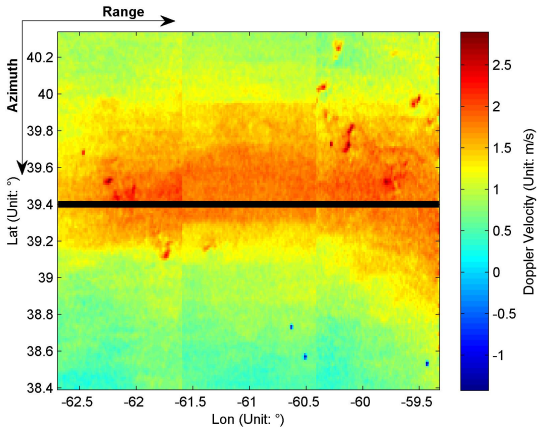

(a)

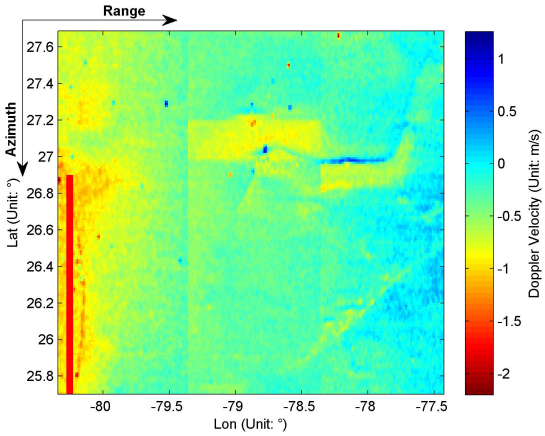

(b)

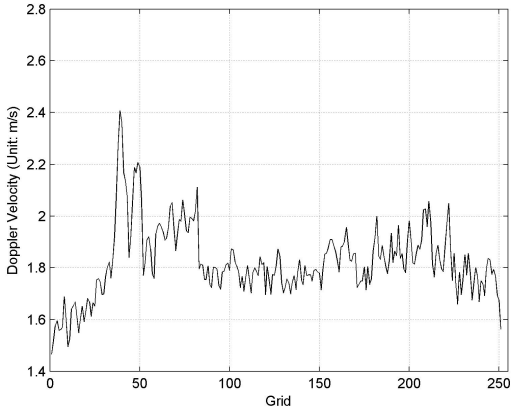

(c)

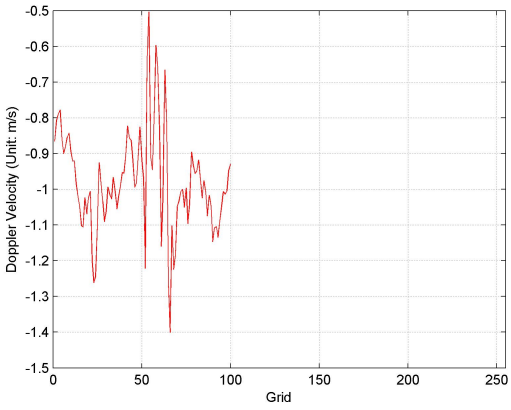

(d)

Figure 5. Sea surface Doppler velocity observations. (a) Doppler velocity image of the Gulf Stream extension region acquired at 22:01 on 07/20/2021 from Sentinel-1 RVL product, with a uniform current in a nearly west-east direction. (b) Doppler velocity image of the Gulf Stream regime off the coast of Florida acquired at 23:20 on 11/07/2021 from Sentinel-1 RVL product, with a uniform current in a nearly north-south direction. (c) The profile along the black line shown in (a). (d) The profile along the red line shown in (b).

4 Conclusions

Through analysis of several examples, we found that the Doppler shift received by the SAR from the echo signal shows different imaging patterns regarding the satellite velocity and sea surface velocity. The difference is determined by the characteristics of the satellite's velocity vector and the sea surface velocity vector at different ground points. As the satellite moves along its orbit round the Earth, the component of the velocity at the ground point is the projection of the satellite's velocity vector, so it exhibits radial characteristics at different observation points. However, the sea surface velocities are different at different sea surface points, which is mainly dominated by the distribution of the dynamic sea surface field, so they do not exhibit any radial features.

The main conclusions of this paper are as follows. (1) The DC linear trends in the azimuth and range directions are caused by the relative motion between the satellite and the Earth. The linear trend in azimuth direction is caused by the linear change of satellite speed in orbit, while the linear trend in the range direction is caused by the projection of the satellite's speed onto the ground, so the radial characteristics can only been seen in the range direction on the $f_{\mathrm{SAT}}^{\mathrm{Rg}}$ image. (2) The Doppler shift caused by the sea surface motion does not exhibit radial features because the electromagnetic waves emitted by spaceborne SAR do not propagate along the radial direction when they are projected onto the sea surface. (3) The concept of the radial velocity established for HF radar is not applicable to spaceborne SAR. The radial velocity measured via spaceborne SAR is the component of the satellite's velocity in the range direction, which is different from the radial sea surface velocity component measured via HF radar. The image of the radial velocity measured via HF radar exhibits a central radial distribution, while the radial satellite velocity image measured via SAR exhibits a strip-like distribution.

Acknowledgments

The authors declare that they have no competing interests. The research was supported by the National Natural Science Foundation of China (Grants 42027805 and 41620104003). The authors also thank the European Space Agency (ESA) and the Copernicus Open Access Hub for providing free Sentinel-1 data. We thank LetPub (www.letpub.com) for its linguistic assistance during the preparation of this manuscript.

Data and materials availability Statement

All of the experimental data and code can be found at https://github.com/opsmith163/opsmith163. The Sentinel-1 satellite data can be found at https://scihub. copernicus.eu/dhus/#/home.

References

Barrick, D.. (1972a). First-order theory and analysis of MF/HF/VHF scatter from the sea. IEEE Transactions on Antennas and Propagation, 20(1), 2-10. https://doi.org/10.1109/TAP.1972.1140123

Barrick, D.. (1972b). Remote sensing of sea state by radar. Remote sensing of the Troposphere, V. E. Derr (Ed.), U.S. Government Printing office, Washington DC.

Barrick, D.. (1978). HF radio oceanography — A review. Boundary-Layer Meteorol 13, 23–43. https://doi.org/10.1007/BF00913860

Barrick D., Evans M., Weber B., Ocean surface currents mapped by radar.*Science*, 198(4313), 138-144. http://dx.doi.org/10.1126/science.198.4313.138

Barrick, D., & Snider, J.. (1977). The statistics of hf sea-echo doppler spectra. *IEEE Journal of Oceanic Engineering*, 2(1), 19-28. https://doi.org/10.1109/TAP.1977.1141529

Chapron, B., Collard, F, Ardhuin, F. (2005). Direct measurements of ocean surface velocity from space: Interpretation and validation. *J. Geophys. Res. 110*, C07008. https://doi.org/10.1029/2004jc002809

Crombie, D. D. (1955). Doppler spectrum of sea echo at 13.56 Mc./s. *Nature 175*, 681-682. https://doi.org/10.1038/175681a0

Cumming, I. G., & Wong, F. H. (Eds.). (2004). *Digital Signal Processing of Synthetic Aperture Radar Data: Algorithms and Implementation*. Fitchburg, MA: Artech house.

Johannessen J. A., Kudryavtsev V., Chapron B., et al. (2006). Backscatter and Doppler Signals of Surface Current in SAR Images: A Step Towards Inverse Modelling. Paper presented at Advances in SAR Oceanography from Envisat and ERS Missions.

Johannessen, J. A., Chapron, B., Collard, F., Kudryavtsev, V., Mouche, A., Akimov, D., Dagestad, K. F. (2008). Direct ocean surface velocity measurements from space: improved quantitative interpretation of envisat asar observations. *Geophys. Res. Lett., **35***, L22608. https://doi.org/10.1029/2008GL035709

Lipa B. and Barrick D.. (1983). Least-squares methods for the extraction of surface currents from CODAR crossed-loop data: Application at ARSLOE. *IEEE Journal of Oceanic Engineering*, 8(4), 226-253. https://doi.org/10.1109/JOE.1983.1145578

Martin A., Gommenginger C., Jacob B., Staneva J..(2022).First multi-year assessment of Sentinel-1 radial velocity products using HF radar currents in a coastal environment. *Remote Sensing of Environment*, 268(112758). https://doi.org/10.1016/j.rse.2021.112758

Mujiasih S., Hartanto D., Beckers J.M., Barth A..(2021). Reducing the error in estimates of the Sunda Strait currents by blending HF radar currents with model results. *Continental Shelf Research*, 228(104512). https://doi.org/10.1016/j.csr.2021.104512

Romeiser, R., Johannessen, J., Chapron, B., Collard, F., Kudryavtsev, V., Runge, H., Suchandt, S. (2010). Direct surface current field imaging from space

by along-track InSAR and conventional SAR. In Barale, V., J. Gower, and L. Alberotanza (Eds.), *Oceanography from Space: Revisited* (pp. 73-91), Dordrecht: Springer Netherlands.

Wait, J. R. (1966). Theory of HF ground wave backscatter from sea waves, *J. Geophys. Res.*,71(20), 4839– 4842. https://doi.org/10.1029/JZ071i020p04839

Wang, L., Gao, Y., Lu, P. et al. (2022). A new Doppler frequency anomaly algorithm for surface current measurement with SAR. *J. Ocean. Limnol.* 40, 470-484. https://doi.org/10.1007/s00343-021-0492-4

Yang, X., He, Y. (2022). Retrieval of a real-time sea surface vector field from SAR Doppler centroid: 1. Ekman current retrieval. *J. Geophys. Res.: Oceans.* (Under review)